Journal of Alloys and Compounds 501 (2010) 177–182

Contents lists available at ScienceDirect

Journal of Alloys and Compounds

journal homepage: www.elsevier.com/locate/jallcom

Giant magnetocaloric and barocaloric effects in $Mn(As_{1-x}Sb_x)$

L.G. de Medeiros Jr.[a], N.A. de Oliveira[a,*], A. Troper[b]

[a] Instituto de Física Armando Dias Tavares, Universidade do Estado do Rio de Janeiro, Rua São Francisco Xavier 524, Rio de Janeiro, 20550-013 RJ, Brazil
[b] Centro Brasileiro de Pesquisas Físicas, Rua Xavier Sigaud 150, Rio de Janeiro, 22290-180 RJ, Brazil

ARTICLE INFO

Article history:
Received 23 March 2010
Accepted 31 March 2010
Available online 8 April 2010

Keywords:
Magnetocaloric effect
Metals and alloys
Thermodynamic modeling

ABSTRACT

In this work, we discuss the magnetocaloric and barocaloric effects in the doped compound $Mn(As_{1-x}Sb_x)$, by using a model based in the framework of the band theory. In this model, the two body interaction is treated in the Hartree–Fock approach and the chemical disorder is treated in the coherent potential approximation. Our theoretically calculated magnetocaloric potentials are in very good agreement with the available experimental data. Besides, our theoretical calculations show that the doped compound $Mn(As_{1-x}Sb_x)$ also exhibits giant barocaloric effect.

1. Introduction

The magnetocaloric effect [1–3] is characterized by the isothermal entropy change ΔS_{iso} and by the adiabatic temperature change ΔT_{ad} upon magnetic field variation. In order to provide a good theoretical description of the magnetocaloric effect in a given compound, we should consider the nature of its magnetism. For instance, in rare earth based compounds, where the magnetism comes entirely from the rare earth ions, the magnetocaloric effect may be described by the model of localized magnetic moments. On the other hand, in transition metals based compounds, where the magnetism comes from the itinerant electrons, the magnetocaloric effect should be discussed through theoretical models in the framework of band theory.

Despite the good theoretical description of the available experimental data of the magnetocaloric potentials ΔS_{iso} and ΔT_{ad}, some important aspects of the magnetocaloric effect are not yet completely understood. Besides, there is a lack of a microscopic description of the effects of doping and applied pressure on the magnetocaloric properties of transition metals based compounds.

In this work, the focus in on the theoretical description of the magnetocaloric and barocaloric effects in the doped compound $Mn(As_{1-x}Sb_x)$. Experimental data of the magnetocaloric effect in this compound can be found in references [4–8]. The magnetocaloric effect in the pure compound MnAs has already been theoretically discussed in the literature, by using a model of itinerant electrons [9]. However, a theoretical description of the magnetocaloric effect in the doped compound $Mn(As_{1-x}Sb_x)$ is not yet available in the literature. In addition, the barocaloric effect in this doped compound has not been studied yet.

The primary objective of this paper is to describe the magnetocaloric and barocaloric effects in the doped compound $Mn(As_{1-x}Sb_x)$, by using a model with two sublattices, in the framework of band theory. The second goal of this paper is to make a comparison between the results of the magnetocaloric potentials, obtained with the two sublattice model and the ones obtained with other models found in the literature. For this purpose, we also calculate the magnetocaloric effect in the doped compound $Mn(As_{1-x}Sb_x)$ by using the following models: (i) the effective band model, similar to that one used in reference [10] to describe the pressure effect on the magnetocaloric effect in $La(Fe_{1-x}Si_x)_{13}$, (ii) the model of localized magnetic moments, similar to that one used in reference [11] to study the magnetocaloric effect in a simple system with two energy levels. The comparison among these three models shows that they are able to fit the experimental data of the magnetocaloric potentials ΔS_{iso} and ΔT_{ad} in the doped compound $Mn(As_{1-x}Sb_x)$. However, only the two sublattice model provides the correct description of the physical process involved in the magnetocaloric effect of this doped compound.

2. Formulation

In order to theoretically describe the magnetic properties and the caloric effects in the doped compound $Mn(As_{1-x}Sb_x)$, we start with the following model Hamiltonian:

$$\mathcal{H} = \mathcal{H}_{mag} + \mathcal{H}_{lat}, \quad (1)$$

* Corresponding author.
E-mail address: nilson@uerj.br (N.A. de Oliveira).

0925-8388/$ – see front matter © 2010 Elsevier B.V. All rights reserved.
doi:10.1016/j.jallcom.2010.03.244

where

$$\mathcal{H}_{\mathrm{mag}} = \sum_{i\sigma} \varepsilon_i^{\mathrm{Mn}} d_{i\sigma}^{+} d_{i\sigma} + \sum_{ij\sigma} T_{ij\sigma}^{\mathrm{MnMn}} d_{i\sigma}^{+} d_{j\sigma} + \sum_{i\sigma} U^{\mathrm{Mn}} n_{i\uparrow}^{\mathrm{Mn}} n_{i\downarrow}^{\mathrm{Mn}} - g^{\mathrm{Mn}} \mu_B \sum_i s_i^{\mathrm{Mn}} B + \sum_{i\sigma} \varepsilon_i^{\lambda} c_{i\sigma}^{+} c_{i\sigma} + \sum_{ij\sigma} T_{ij\sigma}^{\lambda\eta} c_{i\sigma}^{+} c_{j\sigma} + \sum_{ij\sigma} T_{ij\sigma}^{\lambda\mathrm{Mn}} (d_{i\sigma}^{+} c_{j\sigma} + c_{j\sigma} d_{i\sigma}^{+}), \tag{2}$$

$$\mathcal{H}_{\mathrm{lat}} = \sum_q \hbar\omega_q a_q^{+} a_q. \tag{3}$$

The Hamiltonian $\mathcal{H}_{\mathrm{lat}}$ describes the phonons in the crystalline lattice. The Hamiltonian $\mathcal{H}_{\mathrm{mag}}$ describes a system of itinerant electrons with two sublattices. One sublattice (B sublattice) is occupied by the magnetic Mn ions, while the other one (A sublattice) is occupied by the non magnetic As and Sb ions. In the magnetic Hamiltonian, the first term represents the local energy at the Mn sites ($\varepsilon_i^{\mathrm{Mn}}$). The second term describes the electron hopping between two Mn sites, where $T_{ij\sigma}^{\mathrm{MnMn}} = \sum_k \tilde{\varepsilon}_k^{\mathrm{Mn}} \mathrm{e}^{ik(R_i - R_j)}$. Here $\tilde{\varepsilon}_k^{Mn} = \alpha_P^{Mn} \xi^{Mn} \varepsilon_k^{Mn}$ is the electron dispersion relation associated with the B sublattice, where α_P^{Mn} simulates the pressure effect and ξ^{Mn} represents the magnetoelastic coupling. Here we consider $\xi^{\mathrm{Mn}} = [1 - \xi_0^{\mathrm{Mn}} (M^{\mathrm{Mn}})^2]$, where ξ_0^{Mn} is a fixed parameter and M^{Mn} is the magnetization at the Mn sublattice. The third term represents the local Coulomb interaction, where U^{Mn} is a model parameter. The fourth term represents the Zeeman interaction between the Mn magnetic moment and the applied magnetic field. The fifth term represents the local energy ε_i^{λ} (λ = As or Sb) associated with the electrons at the sites of the A sublattice. The sixth term represents the electron hopping between the sites of the same sublattice A, where $T_{ij\sigma}^{\lambda\eta} = \sum_k \varepsilon_k^{\mathrm{A}} \mathrm{e}^{ik(R_i - R_j)}$ with $\varepsilon_k^{\mathrm{A}}$ being the electron dispersion relation associated with the A sublattice. The last term represents the electron hopping between the Mn sites and the sites of the A sublattice, where $T_{ij\sigma}^{\lambda\mathrm{Mn}} = \sum_k \tilde{\gamma} \varepsilon_k^{A} \mathrm{e}^{ik(R_i - R_j)}$ and $\tilde{\gamma}$ is a model parameter. In the mean field approximation, the magnetic Hamiltonian turns out to be:

$$\mathcal{H}_{\mathrm{mag}} = \sum_{i\sigma} \varepsilon_{i\sigma}^{\mathrm{Mn}} d_{i\sigma}^{+} d_{i\sigma} + \sum_{ij\sigma} T_{ij\sigma}^{\mathrm{MnMn}} d_{i\sigma}^{+} d_{j\sigma} + \sum_{i\sigma} \varepsilon_i^{\lambda} c_{i\sigma}^{+} c_{i\sigma} + \sum_{ij\sigma} T_{ij\sigma}^{\lambda\eta} c_{i\sigma}^{+} c_{j\sigma} + \sum_{ij\sigma} T_{ij\sigma}^{\lambda\mathrm{Mn}} (d_{i\sigma}^{+} c_{j\sigma} + c_{j\sigma} d_{i\sigma}^{+}), \tag{4}$$

where $\varepsilon_{i\sigma}^{\mathrm{Mn}} = \varepsilon_i^{\mathrm{Mn}} + U^{\mathrm{Mn}} \left\langle n_{i-\sigma}^{\mathrm{Mn}} \right\rangle - \sigma B$ is a renormalized energy. In order to treat the chemical disorder we use the Coherent Potential Approximation (CPA). In this approach, where the disorder is replaced by an effective atom with self energy Σ^{A}, the magnetic Hamiltonian reads:

$$\mathcal{H}_{\mathrm{mag}}^{(0)} = \sum_{i\sigma} \varepsilon_{i\sigma}^{\mathrm{Mn}} d_{i\sigma}^{+} d_{i\sigma} + \sum_{ij\sigma} T_{ij\sigma}^{\mathrm{MnMn}} d_{i\sigma}^{+} d_{j\sigma} + \sum_{i\sigma} \Sigma_{\sigma}^{\mathrm{A}} c_{i\sigma}^{+} c_{i\sigma} + \sum_{ij\sigma} T_{ij\sigma}^{\mathrm{AA}} c_{i\sigma}^{+} c_{j\sigma} + \sum_{ij\sigma} T_{ij\sigma}^{\mathrm{MnA}} (d_{i\sigma}^{+} c_{j\sigma} + c_{j\sigma} d_{i\sigma}^{+}). \tag{5}$$

In order to simplify the calculations of the Green's functions associated with the previous Hamiltonian, we use the homothetic band approximation. In this approach, we take $\varepsilon_k^{\mathrm{A}} = \varepsilon_k$, where ε_k is a reference dispersion relation. The dispersion relation associated with the Mn sublattice is taken proportional to this one, i.e., $\varepsilon_k^{\mathrm{Mn}} = \alpha^{\mathrm{Mn}} \varepsilon_k$. In this way, the renormalized dispersion relation $\tilde{\varepsilon}_k^{\mathrm{Mn}} = \alpha_P^{\mathrm{Mn}} \xi^{\mathrm{Mn}} \varepsilon_k^{\mathrm{Mn}}$ takes the form $\tilde{\varepsilon}_k^{\mathrm{Mn}} = \tilde{\alpha}^{\mathrm{Mn}} \varepsilon_k$, where $\tilde{\alpha}^{\mathrm{Mn}} = \alpha_P^{\mathrm{Mn}} \alpha^{\mathrm{Mn}} \xi^{\mathrm{Mn}}$. Within this approximation, the Green's functions for the Hamiltonian in Eq. (5) are given by:

$$g_{ii}^{\mathrm{AA}}(z) = \frac{1}{(\tilde{\alpha}^{\mathrm{Mn}} - \tilde{\gamma}^2)(E_+^{\sigma} - E_-^{\sigma})} [(z - \varepsilon_{\sigma}^{\mathrm{Mn}} - \tilde{\alpha}^{\mathrm{Mn}} E_-^{\sigma}) F(E_-^{\sigma}) - (z - \varepsilon_{\sigma}^{\mathrm{Mn}} - \tilde{\alpha}^{\mathrm{Mn}} E_+^{\sigma}) F(E_+^{\sigma})] \tag{6}$$

$$g_{ii}^{\mathrm{MnMn}}(z) = \frac{1}{(\tilde{\alpha}^{\mathrm{Mn}} - \tilde{\gamma}^2)(E_+^{\sigma} - E_-^{\sigma})} [(z - \Sigma_{\sigma}^{A} - E_-^{\sigma}) F(E_-^{\sigma}) - (z - \Sigma_{\sigma}^{A} - E_+^{\sigma}) F(E_+^{\sigma})], \tag{7}$$

where

$$E_{\pm}^{\sigma} = \frac{1}{2(\tilde{\alpha}^{\mathrm{Mn}} - \tilde{\gamma}^2)} \{ [\tilde{\alpha}^{\mathrm{Mn}} (z - \Sigma_{\sigma}^{\mathrm{A}}) + (z - \varepsilon_{\sigma}^{\mathrm{Mn}})] \pm \{ [\tilde{\alpha}^{\mathrm{Mn}} (z - \Sigma_{\sigma}^{\mathrm{A}}) + (z - \varepsilon_{\sigma}^{\mathrm{Mn}})]^2 - 4(z - \Sigma_{\sigma}^{\mathrm{A}})(z - \varepsilon_{\sigma}^{\mathrm{B}})(\tilde{\alpha}^{\mathrm{B}} - \tilde{\gamma}^2) \}^{1/2} \}. \tag{8}$$

Here $z = \varepsilon + i0$ and $F(E_{\pm}^{\sigma})$ is given by:

$$F(E_{\pm}^{\sigma}) = \int \frac{\rho(\varepsilon)}{E_{\pm}^{\sigma} - \varepsilon} \, \mathrm{d}\varepsilon. \tag{9}$$

Note that the Green's function for the Mn sublattice, depends on the self energy of the A sublattice. As a result, the magnetic properties associated with the Mn sublattice depend on the impurity concentration at the non magnetic A sublattice. In order to determine the self energy $\Sigma_{\sigma}^{\mathrm{A}}$, we introduce in a given site (site 0) of the A sublattice an effective atom with energy $\varepsilon_{\sigma}^{\lambda}$ (λ = As or Sb), creating an impurity problem. Then, to recover the translational invariance we add the terms $\pm \Sigma_{\sigma}^{\mathrm{A}} c_{0\sigma}^{+} c_{0\sigma}$ at the impurity site, so that the Hamiltonian for the impurity problem may be written as:

$$\mathcal{H}_{\mathrm{mag}} = \sum_{l\sigma} \varepsilon_{l\sigma}^{\mathrm{Mn}} d_{l\sigma}^{+} d_{l\sigma} + \sum_{lm\sigma} T_{lm\sigma}^{\mathrm{MnMn}} d_{l\sigma}^{+} d_{m\sigma} + \sum_{il\sigma} T_{il\sigma}^{\mathrm{AMn}} (d_{i\sigma}^{+} c_{l\sigma} + d_{l\sigma} c_{i\sigma}^{+}) + \sum_{i\sigma} \Sigma_{\sigma}^{\mathrm{A}} c_{i\sigma}^{+} c_{i\sigma} + \sum_{ij\sigma} T_{ij\sigma}^{\mathrm{AA}} c_{i\sigma}^{+} c_{j\sigma} + (\varepsilon_{0\sigma}^{\lambda} - \Sigma_{\sigma}^{\mathrm{A}}) c_{0\sigma}^{+} c_{0\sigma}. \tag{10}$$

The previous Hamiltonian has the form $\mathcal{H}_{\mathrm{mag}} = \mathcal{H}_{\mathrm{mag}}^{(0)} + V_{0i}^{\lambda}$, where $\mathcal{H}_{\mathrm{mag}}^{(0)}$ describes the Hamiltonian of the pure system with an effective medium at the A sublattice (see Eq. (5)) and $V_{0i}^{\lambda} = (\varepsilon_{0\sigma}^{\lambda} - \Sigma_{\sigma}^{\mathrm{A}}) c_{0\sigma}^{+} c_{0\sigma}$ is a local potential at the A sublattice. Neglecting the terms of second order, the local perturbed Green's function $G_{00\sigma}^{\mathrm{MnMn}}$ associated with the Hamiltonian in Eq. (10) is given by $G_{00\sigma}^{\mathrm{MnMn}} = g_{00\sigma}^{\mathrm{MnMn}}$, where $g_{00\sigma}^{\mathrm{MnMn}}$ is the local unperturbed Green's function given in Eq. (7). The perturbed Green's function $G_{ij\sigma}^{\lambda\lambda}$ associated with the Hamiltonian (10), is given by:

$$G_{ij\sigma}^{\lambda\lambda}(z) = g_{ij\sigma}^{\mathrm{AA}}(z) + g_{i0\sigma}^{\mathrm{AA}}(z) \left[\frac{V_0^{\lambda}}{1 - g_{00\sigma}(z) V_0^{\lambda}} \right] g_{0j\sigma}^{\mathrm{AA}}(z). \tag{11}$$

Taking the average and imposing the condition $\left\langle G_{ij\sigma}^{\mathrm{AA}}(z) \right\rangle = \left\langle g_{ij\sigma}^{\mathrm{AA}}(z) \right\rangle$ we get the following CPA equation

$$\left\langle \frac{V_0^{\lambda}}{[1 - g_{00\sigma}^{\mathrm{AA}}(z) V_0^{\lambda}]} \right\rangle = 0, \tag{12}$$

which determines the self energy $\Sigma_\sigma^{\mathrm{A}}$. The local perturbed Green's function at the impurity site, calculated from Eq. (11) is given by:

$$G_{00\sigma}^{\lambda\lambda}(z) = \frac{g_{00\sigma}^{\mathrm{AA}}(z)}{1 - g_{00\sigma}^{\mathrm{AA}}(z)V_0^{\lambda}}. \tag{13}$$

The densities of states are given by $\rho_\sigma^{\mathrm{Mn}}(\varepsilon) = -\frac{1}{\pi}\int \mathrm{Im} g_{00\sigma}^{\mathrm{Mn}}(z)\,\mathrm{d}z$ and $\rho_\sigma^{\mathrm{A}}(\varepsilon) = (1-x)\rho_\sigma^{\lambda}(\varepsilon) + x\rho_\sigma^{\eta}(\varepsilon)$, where $\rho_\sigma^{\lambda}(\varepsilon) = -\frac{1}{\pi}\int \mathrm{Im} G_{00\sigma}^{\lambda\lambda}(z)\,\mathrm{d}z$, with $\lambda = \mathrm{As}$ or Sb. The magnetization at the Mn sublattice is determined by $M^{\mathrm{Mn}} = (n_\uparrow^{\mathrm{Mn}} - n_\downarrow^{\mathrm{Mn}})$, where $n_\sigma^{\mathrm{Mn}} = \int f(\varepsilon)\rho_\sigma^{\mathrm{Mn}}\,\mathrm{d}\varepsilon$. The magnetization at the A sublattice is neglected. The partition function associated with the two sublattice Hamiltonian in Eq. (5) is given by:

$$Z_{\mathrm{mag}}(T,B,P) = \prod \left[\sum_{n_{k\sigma}} \mathrm{e}^{-\beta(\varepsilon_{k\sigma}^{\mathrm{Mn}}-\mu)n_{k\sigma}^{\mathrm{Mn}}}\right]\left[\sum_{n_{k\sigma}} \mathrm{e}^{-\beta(\Sigma_{k\sigma}^{\mathrm{A}}-\mu)n_{k\sigma}^{\mathrm{A}}}\right], \tag{14}$$

where $\beta = 1/k_BT$, with k_B being the Boltzmann constant. The free energy is given by $F_{\mathrm{mag}} = (-1/\beta)\ln Z_{\mathrm{mag}}$. The magnetic entropy calculated from $S_{\mathrm{mag}}(T,B,P) = -[\partial F_{\mathrm{mag}}(T,B,P)/\partial T]_B$ is given by:

$$\begin{aligned} S_{\mathrm{mag}}(T,B,P) = \Re\sum_\sigma \Bigg\{ & \int_{-\infty}^{\infty} \ln[1+\mathrm{e}^{-\beta(\varepsilon_\sigma^{\mathrm{Mn}}-\mu)}]\rho_\sigma^{\mathrm{Mn}}(\varepsilon)\,\mathrm{d}\varepsilon \\ & + \frac{1}{k_BT}\int_{-\infty}^{\infty}(\varepsilon_\sigma^{\mathrm{Mn}}-\mu)\rho_\sigma^{\mathrm{Mn}}(\varepsilon)f(\varepsilon)\,\mathrm{d}\varepsilon \\ & + \int_{-\infty}^{\infty}\ln[1+\mathrm{e}^{-\beta(\Sigma_\sigma^{\mathrm{A}}-\mu)}]\rho_\sigma^{\mathrm{A}}(\varepsilon)\,\mathrm{d}\varepsilon \\ & + \int_{-\infty}^{\infty}(\Sigma_\sigma^{\mathrm{A}}-\mu)\rho_\sigma^{\mathrm{A}}(\varepsilon)f(\varepsilon)\,\mathrm{d}\varepsilon \Bigg\}, \end{aligned} \tag{15}$$

where $\Re$ is the gas constant. The total entropy is given by $S = S_{\mathrm{mag}} + S_{\mathrm{lat}}$, where S_{mag} is the magnetic entropy given in the previous equation and S_{lat} is the entropy of the crystalline lattice taken in the Debye approximation [3]. The magnetocaloric potentials are calculated by $\Delta S_{\mathrm{iso}}(T, B_2 - B_1, P) = S(T, B_2, P) - S(T, B_1, P)$ and by $\Delta T_{\mathrm{ad}}(T, B_2 - B_1, P) = T_2(B_2) - T_1(B_1)$, under the adiabatic condition $S(T_2, B_2, P) = S(T_1, B_1, P)$. The barocaloric potentials are calculated by $\Delta S_{\mathrm{iso}}^{\mathrm{bar}}(T, B, P_2 - P_1) = S(T, B, P_2) - S(T, B, P_1)$ and by $\Delta T_{\mathrm{ad}}^{\mathrm{bar}}(T, B, P_2 - P_1) = T_2(P_2) - T_1(P_1)$, under the adiabatic condition $S(T_2, B, P_2) = S(T_1, B, P_1)$.

3. Results and discussion

In this section, we apply the two sublattice model to calculate the magnetocaloric and barocaloric effects in the doped compound $\mathrm{Mn(As_{1-x}Sb_x)}$ for $x = 0$, 0.1 and 0.3. For this purpose, we adopt a model density of states with 0.7593 eV of bandwidth. The homothetic band parameters were taken as $\alpha^{\mathrm{Mn}} = 0.90$; and $\tilde{\gamma} = 0.01, 0.03$ and 0.05, for $x = 0$, 0.1 and 0.3 respectively. The Coulomb interaction parameter was taken as $U^{\mathrm{Mn}} = 0.38$ in units of the bandwidth. The magnetoelastic coupling parameter was taken as $\xi_0^{\mathrm{Mn}} = 0.91$, 0.85 and 0.75 for $x = 0$, 0.1 and 0.3 respectively. The Debye temperature was taken as 400 K for any impurity concentration. The initial numbers of electrons at the crystalline lattice sites were taken as $n^{\mathrm{As}} = n^{\mathrm{Sb}} = 1.2$ and $n^{\mathrm{Mn}} = 6.85$. It should be emphasized that the final electron occupation numbers at Mn, As and Sb sites depend on the impurity concentration and are self-consistently determined.

For the sake of comparison, we also calculate the magnetic properties and the magnetocaloric effect in the doped compound $\mathrm{Mn(As_{1-x}Sb_x)}$, by using the following models: (i) the effective band model, similar to that one used in reference [10]. (ii) The model of localized magnetic moments, similar to that one discussed in reference [11]. Technical details about these models can be found in the mentioned references. Here, we just present the main parameters used in the calculations. In the case of the effective band model, we adopt the same electron occupation numbers used in the case of the two sublattice model. However, it should be mentioned that in the effective band model, the electron occupation number at the Mn sites is always the same, independently of the Sb concentration. The Coulomb interaction parameter U^{Mn} was chosen in order to reproduce the magnetization at $T = 0\,K$. In this effective band model, the effect of the impurity concentration on the magnetic properties is considered via the renormalization of the ratio U^{Mn}/W, where W is the energy bandwidth. In the case of the model of localized magnetic moments, we consider the effective angular momentum as $J = 2.5$ and the Landé factor as $g = 1.65$. The effective exchange interaction integral parameter ($\mathcal{J}_0$) and the magnetoelastic coupling parameters ($\mathcal{J}_1$) were suitably chosen to reproduce the experimental data of the magnetic ordering temperature, as a function of impurity concentration (see reference [11] for details about the model parameters).

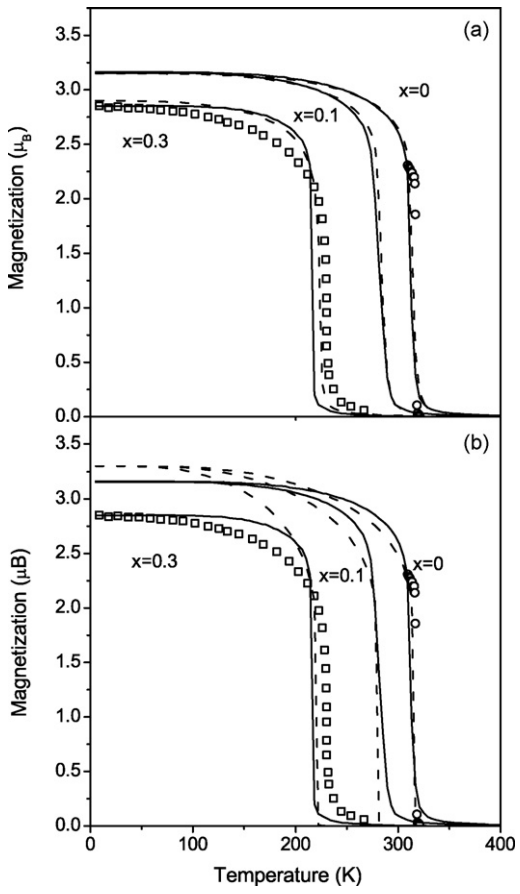

Fig. 1. Temperature dependence of the magnetization in $\mathrm{Mn(As_{1-x}Sb_x)}$. The solid lines represent the calculations using the two sublattice model, while symbols represent experimental data [5,8]. The dashed lines represent the calculations using the effective band model (a) and the model of localized magnetic moments (b).

In Fig. 1a, we plot the temperature dependence of the magnetization in $\mathrm{Mn(As_{1-x}Sb_x)}$ at ambient pressure. In this figure, the solid lines represent the calculations obtained with the two sublattice model, while the dashed lines represent the corresponding calculations using the effective band model. Note that both itinerant models describe quite well the available experimental data of magnetization, represented in this figure by symbols [5,8]. In Fig. 1b, we plot the magnetization at ambient pressure obtained with the two sublattice model (solid lines), together with the corresponding cal-

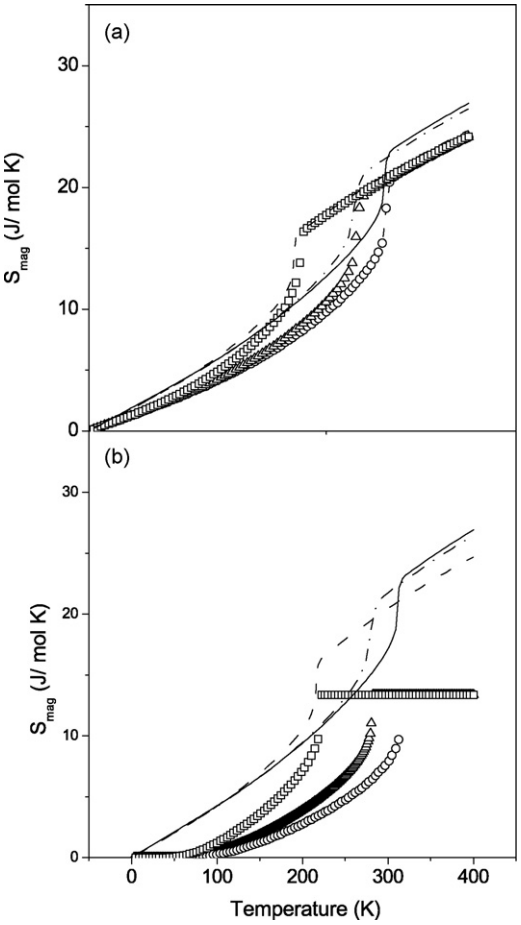

Fig. 2. Magnetic entropy in $Mn(As_{1-x}Sb_x)$ for $B = 0$. The solid, dashed-dotted and dashed lines represent the calculations using the two sublattice model for $x = 0$, 0.1 and 0.3 respectively. Open circles, triangles and squares represent the corresponding calculations using the effective band model (a) and the model of localized moments (b).

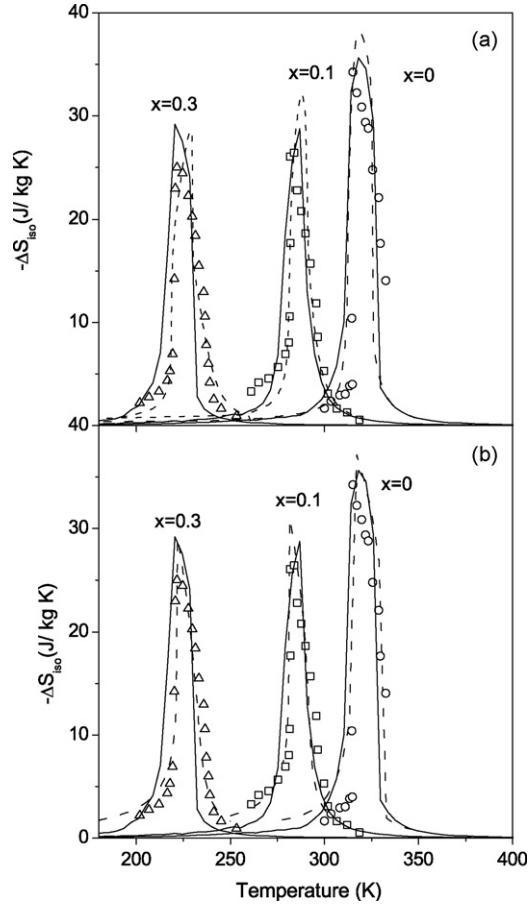

Fig. 3. Magnetocaloric potential ΔS_{iso} in $Mn(As_{1-x}Sb_x)$ upon magnetic field variation from 0 to 5 T. The solid lines represent the calculations of the two sublattice model while symbols are experimental data [6]. The dashed lines represent the calculations obtained with the effective band model (a) and the model of localized magnetic moments (b).

culations using the model of localized magnetic moments(dashed line). From this figure, we can observe that the model of localized magnetic moments is also able to reproduce the magnetic ordering temperature, as a function of impurity concentration. However, it fails to explain the reduction of the magnetization at $T = 0$ K, as a function of impurity concentration. Note that the magnetization at $T = 0$ *K*, calculated with the model of localized magnetic moments is always the same, i.e., $M(0) = gJ$, independently of the impurity concentration. This discrepancy between theory and experiment, which is well known in the literature, indicates one of the limitations of the model of localized magnetic moments to describe the magnetic properties of transitions metals based compounds.

In Fig. 2a, we plot the magnetic part of the entropy at ambient pressure and for $B = 0$, calculated using both the two sublattice model (lines) and the effective band model(open symbols). From Fig. 2a, we can observe that the magnetic entropy calculated with the effective band model, saturates at high temperatures at the same value. This is due to the fact that in this model the electron occupation number at the Mn site is always the same, independently of the impurity concentration. On the other hand, in the case of the two sublattice model, the values of the magnetic entropy at high temperatures depend on the impurity concentration. This is due to the fact that in the two sublattice model, the electron occupation number at the Mn site changes as a function of impurity concentration. As a matter of fact, in the doped compound $Mn(As_{1-x}Sb_x)$, the charge transfer between Mn and the As–Sb sites is the main physical mechanism behind the magnetocaloric properties as a function of impurity concentration. In Fig. 2b, we plot the magnetic part of the entropy at ambient pressure and for $B = 0$, calculated using the two sublattice model (lines) together with the corresponding calculations using the model of localized magnetic moments (open symbols). From this figure, we can observe that the saturation value of the magnetic entropy calculated with the model of localized magnetic moments, which is determined by the relation $\Re \ln(2J + 1)$, is smaller than the one calculated using the two sublattice model. This discrepancy is another indication that the model of localized magnetic moments is not appropriate to correctly describe the magnetocaloric effect in transition metals based compounds.

In Fig. 3a, we plot the isothermal entropy changes at ambient pressure and upon magnetic field variation from 0 to 5 *T*, calculated using both the two sublattice model (solid lines) and the effective band model (dashed lines). In Fig. 3b, we plot the isothermal entropy changes at ambient pressure and upon magnetic field variation from 0 to 5 T calculated using both the two sublattice model and the model of localized magnetic moments. The corresponding calculations for the adiabatic temperature changes are plotted in Fig. 4a and b. From Figs. 3 and 4, we can observe that the magnetocaloric potentials calculated using the three different models are in very good agreement with the available experimental data [6].

The results shown in this paper point out that: (1) the two sublattice model enables us to perform a systematic description of the experimental data of the magnetization and the magnetocaloric

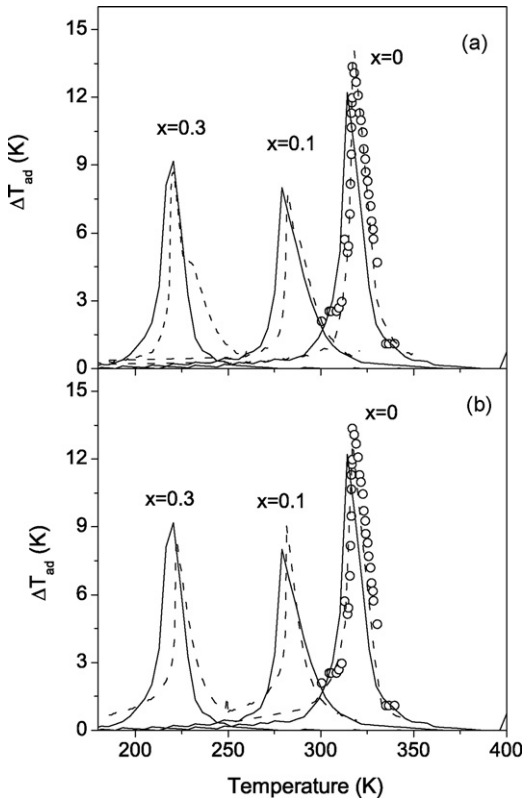

Fig. 4. Magnetocaloric potential ΔT_{ad} in $Mn(As_{1-x}Sb_x)$ upon magnetic field variation from 0 to 5 T. The solid lines represent the calculations obtained with the two sublattice model while symbols are the available experimental data [4]. The dashed lines represent the calculations using the effective band model (a) and the model of localized magnetic moments (b).

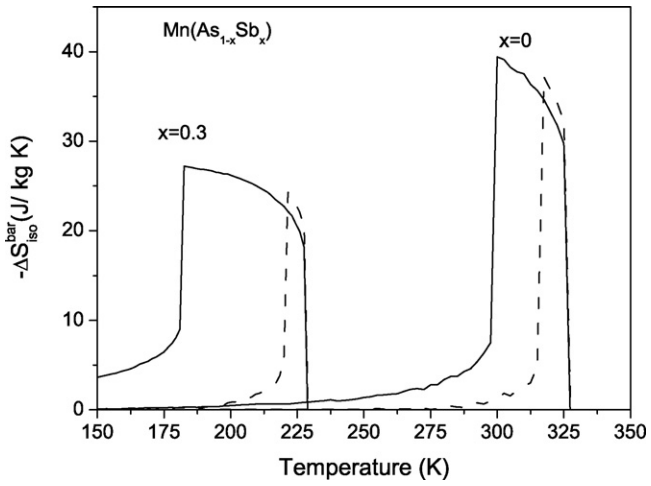

Fig. 5. Barocaloric potential ΔS_{iso}^{bar} (solid lines) in $Mn(As_{1-x}Sb_x)$, calculated for $B = 1\ T$ and upon pressure variation from p_1 to p_0 (case of $x = 0$)and from p_2 to p_0 (case of $x = 0.3$). The dashed lines represent the magnetocaloric potential ΔS_{iso}, calculated at ambient pressure and upon magnetic field variation from 0 to 1 T.

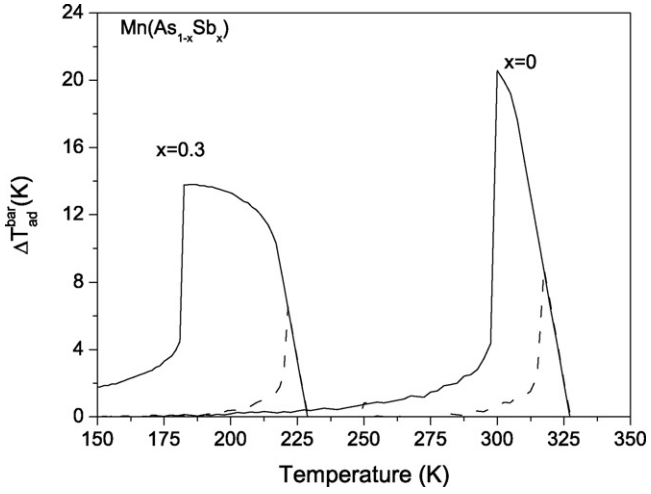

Fig. 6. Barocaloric potential ΔT_{ad}^{bar} (solid lines) in $Mn(As_{1-x}Sb_x)$, calculated for $B = 1$ T and upon pressure variation from p_1 to p_0 (case of $x = 0$)and from p_2 to p_0 (case of $x = 0.3$). The dashed lines represent the magnetocaloric potential ΔT_{ad}, calculated at ambient pressure and upon magnetic field variation from 0 to 1 T.

effect in the doped compound $Mn(As_{1-x}Sb_x)$. (2) The effective band model also yields reasonable values for magnetization and magnetocaloric potentials in the doped compound $Mn(As_{1-x}Sb_x)$. However, the electron transfer between the lattice sites, due to the process of doping is not well considered in the effective band model. (3) The model of localized magnetic moments fails to explain the magnetic and the thermodynamic properties of the doped compound $Mn(As_{1-x}Sb_x)$. Nevertheless, it also provides very reasonable values for the magnetocaloric potentials ΔS_{iso} and ΔT_{ad} in this doped compound. This fact indicates that the model of localized magnetic moments may be used as a first attempt to get an estimate of the magnetocaloric potentials in transition metal based compounds with the usual behavior. However, the model of localized magnetic moments should not be used to draw conclusions about new features of the magnetocaloric effect in transition metals based compounds.

We also use the two sublattice model to calculate the barocaloric effect in the doped compound $Mn(As_{1-x}Sb_x)$. In order to illustrate our calculations, we show the barocaloric potentials in the pure compound MnAS upon pressure variation from p_1 to p_0 and in the doped compound $Mn(As_{0.7}Sb_{0.3})$ from p_2 to p_0. Here p_0 is the ambient pressure, p_1 is an external pressure around 1.5 kbar, which brings the magnetic ordering temperature of the pure compound MnAs to 295 K and p_2 is an external pressure around 10 kbar, which brings the magnetic ordering temperature of the compound $Mn(As_{0.7}Sb_{0.3})$ to 160 K. In the model, these values of external pressure were simulated by the parameter $\alpha_P^{Mn} = 1.02$. The calculated barocaloric potentials ΔS_{iso}^{bar} and ΔT_{ad}^{bar} are shown by the solid lines in Figs. 5 and 6 respectively. For the sake of comparison, we also plot in these figures the magnetocaloric potentials ΔS_{iso} and ΔT_{ad} calculated at ambient pressure and upon magnetic field variation from 0 to 1 T. From these figures, we can observe that the doped compound $Mn(As_{1-x}Sb_x)$ exhibits giant barocaloric effect in a wide range of temperatures. This fact points out that the giant barocaloric effect in the doped $Mn(As_{1-x}Sb_x)$, which need experimental data to be confirmed, is very important to construct cooling devices based on the barocaloric effect. To conclude this paper, we want to emphasize that the giant barocaloric effect is expected to occur in any other magnetic compound undergoing a first order phase transition.

Acknowledgements

We acknowledge financial support from CNPq and FAPERJ.

References

[1] A.M. Tishin, Y.I. Spichkin, The Magnetocaloric Effect and its Applications, Institute of Physics, Bristol and Philadelphia, 2003.
[2] K.A. Gschneidner Jr., V.K. Pecharsky, A.O. Tsokol, Rep. Prog. Phys. 68 (2005) 1479–1539.
[3] N.A. de Oliveira, P.J. von Ranke, Phys. Rep. 489 (2010) 89–159.
[4] H. Wada, Y. Tanabe, Appl. Phys. Lett. 79 (2001) 3302–3304.

[5] H. Wada, K. Taniguchi, Y. Tanabe, Mater. Trans. 43 (2002) 73–77.
[6] H. Wada, T. Morikawa, K. Taniguchi, T. Shibata, Y. Yamada, Y. Akishige, Phys. B 328 (2003) 114–116.
[7] H. Wada, S. Matsuo, A. Mitsuda, Phys. Rev. B 79 (2009) 092407.
[8] T. Goto, M.I. Bartashevich, K. Kondo, K. Terao, H. Yamada, H. Ido, J. Alloys Compd. 325 (2001) 18–23.
[9] N.A de Oliveira, Eur. Phys. J. B 40 (2004) 259–264.
[10] L.G. de Medeiros Jr., N.A. de Oliveira, A. Troper, J. Appl. Phys. 103 (2008) 113909.
[11] N.A. de Oliveira, P.J. von Ranke, Phys. Rev. B 77 (2008) 214439.